International Global Navigation Satellite Systems Society
IGNSS Symposium 2009

Holiday Inn Surfers Paradise, Qld, Australia
1 – 3 December, 2009

Fast LAMBDA-based ambiguity resolution combined with WARTK technique for Galileo data simulated using ESA's Galileo Signal Validation Facility

Dennis Odijk (1)
Department of Spatial Sciences, Curtin University of Technology, Australia
Tel: +61 8 9266 3369, Fax: +61 9266 2703, Email: d.odijk@curtin.edu.au
Peter de Bakker (2)
Delft Institute of Earth Observation & Space Systems, Delft University of Technology, The Netherlands
Tel: +31 15 278 2569, Fax: +31 15 278 3711, Email: p.f.debakker@tudelft.nl
Sandra Verhagen (3)
Delft Institute of Earth Observation & Space Systems, Delft University of Technology, The Netherlands
Tel: +31 15 278 4545, Fax: +31 15 278 3711, Email: a.a.verhagen@tudelft.nl
Peter J.G. Teunissen (4)
Department of Spatial Sciences, Curtin University of Technology, Australia
Tel: +61 8 9266 7676, Fax: +61 9266 2703, Email: p.teunissen@curtin.edu.au
Delft Institute of Earth Observation & Space Systems, Delft University of Technology, The Netherlands
Tel: +31 15 278 3546, Fax: +31 15 278 3711, Email: p.j.g.teunissen@tudelft.nl
Manuel Hernández-Pajares (5)
Research Group of Astronomy and Geomatics, Technical University of Catalonia (gAGE/UPC), Spain
Tel: +34 93 4016029, Fax: +34 93 4015981, Email: manuel@ma4.upc.edu
Jaron Samson (6)
ESA/ESTEC, Noordwijk, The Netherlands
Tel: +31 71 565 6591, Fax: +31 71 565 4596, Email: jaron.samson@esa.int

ABSTRACT

This contribution addresses the effect of having a triple frequency Global Navigation Satellite System (GNSS) on ambiguity resolution of long baselines, i.e. baselines for which the differential ionospheric delays cannot be ignored. Although it is recognized that a combination of GNSS's is more effective for integer ambiguity resolution –the key to highly accurate positioning– than the use of three frequencies, it is still of interest to investigate single GNSS triple-frequency ambiguity resolution, especially since it is expected that the quality of the code data of Galileo triple-frequency signals will be better than of current dual-frequency GPS. For this purpose we have simulated triple-frequency Galileo signals using ESA's Galileo Signal Validation Facility for a Wide Area network of permanent stations and user stations receiving Wide Area RTK (WARTK) ionospheric corrections from this network. The three user stations are located at 100-400 km from the network's master reference station. Applying the ionospheric corrections by means of simple ionosphere-weighted processing demonstrated that instantaneous LAMBDA-based ambiguity resolution is

feasible for the 100-km user baseline. However, as a result –in this simple approach– of poorer ionospheric corrections for the longer baselines, the instantaneous success rates drop to close to 0%, even using triple-frequency data. Despite this, the availability of a third frequency is beneficial in reducing the mean ambiguity initialization time when more epochs are used; depending on the noise levels of the code data the times to first fix the ambiguities are in the order of 10-50 sec for the 400-km baseline, applying the WARTK ionospheric corrections.

KEYWORDS: GNSS, Galileo, Triple-Frequency, Ambiguity Resolution, Wide Area RTK, LAMBDA method, GSVF simulator

1. INTRODUCTION

In the near future various Global Navigation Satellite Systems (GNSS) will broadcast signals on three or even four frequencies. The modernized GPS will be extended with the L5 frequency (this is implemented in the newer satellites, e.g. PRN05), while Galileo's Open Service will broadcast signals on the L1, E5a and E5b frequencies. This availability of more signals may be beneficial for high-precision (cm-level) relative positioning, since the performance of carrier phase ambiguity resolution will be improved.

The addition of a third frequency will in principle lead to higher ambiguity success rates since the float ambiguity solution becomes more accurate as a result of having more observations. For short baselines, for which the differential ionospheric delays need not be modelled, this indeed will enable reliable instantaneous (single-epoch) ambiguity resolution at nearly 100% of the time (especially with Galileo), (Verhagen et al., 2007). For longer baselines however, the ionosphere modelling will still remain the limiting factor, implying that instantaneous triple-frequency ambiguity resolution will not be feasible. Much better long baseline performance is expected when GPS is combined with Galileo, since this approximately doubles the number of available satellites.

Despite that triple-frequency long-baseline ambiguity resolution based on just one GNSS and one single epoch is not expected to be highly reliable, it is still of interest to investigate to what extent ambiguity resolution based on triple frequency Galileo is likely to improve compared to current dual-frequency GPS. This is mainly because the Galileo signals are expected to be of higher precision than their GPS counterparts, especially the code measurements (Simsky et al., 2006). In addition, the planned Galileo satellite constellation is more favourable than GPS from an ambiguity resolution point of view, because the number of satellites tracked with Galileo is generally higher than with GPS (Verhagen et al., 2007).

To investigate the expected performance of future Galileo long baseline ambiguity resolution we have simulated triple-frequency phase and code observations using the Galileo Signal Validation Facility (GSVF) at ESA premises. Since a prerequisite for fast long baseline ambiguity resolution is that accurate ionospheric corrections are available, data for a Wide Area RTK (WARTK) network of reference stations at distances between 300 and 1300 km from each other have also been generated. Data of three WARTK user stations, at distances of 114, 257 and 398 km from the master reference station of the network have been simulated.

The remainder of this paper is set up as follows. Section 2 briefly reviews the principles of RTK positioning in the presence of a Wide Area network. In Section 3 we elaborate upon the

applied LAMBDA-based processing strategy for users receiving ionospheric corrections of the Wide Area network. Section 4 explains how the triple-frequency Galileo data have been simulated, while the following section presents the results with respect to the performance of ambiguity resolution for users when applying the WARTK ionospheric corrections generated from the simulated network to their data. Section 6 ends the paper with conclusions.

2. PRINCIPLE OF WIDE-AREA RTK (WARTK) POSITIONING

Wide-Area Real-Time Kinematic (WARTK) is a Network-RTK technique which aims to extend the baseline distance limit of the conventional RTK surveying technique. Depending on the ionospheric conditions at hand, the baseline length is restricted to about 10 km using conventional RTK surveying techniques. Above this distance a user should correct his phase and code data for the ionospheric delays, and these ionospheric corrections should be sufficiently precise, enabling fast ambiguity resolution and positioning with sub-dm accuracy. A characteristic of the WARTK technique is its tomography-based modelling of the ionospheric delays as estimated from the phase data of the network of reference stations (Colombo et al., 1999 and Hernández-Pajares et al., 2004). Using this, very precise ionospheric corrections can be generated in real-time from a reference network with relatively large station spacing (ranging from a few hundred to more than thousand km).

In Hernández-Pajares et al. (2008) it was investigated whether WARTK positioning would be feasible based on the network of Receiver Independent Monitoring Stations (RIMS) of EGNOS (the European SBAS). This RIMS network has stations distributed over the European continent with inter distances of many hundreds of kilometres, see Figure 1. In this feasibility study some of the RIMS stations were selected to generate WARTK ionospheric corrections. As such, the Galileo simulation study as described in this paper was part of this feasibility study.

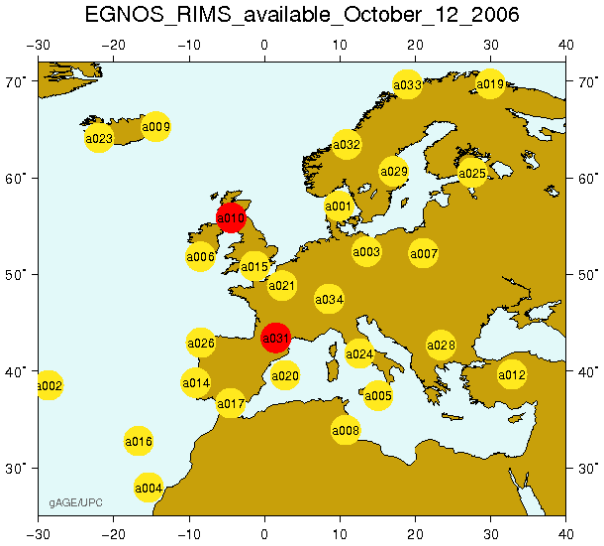

Figure 1 Distribution of EGNOS RIMS stations in Europe.

3. LAMBDA-BASED PROCESSING STRATEGY FOR WARTK USERS

In this section we describe the strategy applied to process the WARTK user data. Although in

Network RTK practice a user will apply a network correction strategy based on either the Virtual Reference Station concept (VRS), see (Vollath et al., 2000) or the Master Auxiliary Concept (MAC), see (Euler et al., 2001) to apply the network corrections to the data, for the purpose of this paper these corrections were directly applied to the observations at both the user and the master reference station of the network.

The user's processing strategy can then be described as follows. The basis of the processing is the ionosphere-weighted GNSS model for relative positioning (Odijk, 2000). The advantage of this model is that it allows the WARTK ionospheric corrections to be incorporated as double-differenced (DD) observations and hence their uncertainty can be accounted for through the stochastic model, in addition to the uncertainty of the multi-frequency DD phase and code observations. The unknown parameters of the model are formed by the relative baseline (coordinate) components, zenith tropospheric delay (if necessary), DD ionospheric delays and the DD ambiguities. It is mentioned that when the standard deviations of the DD ionospheric observations are set to zero, the ionosphere-weighted model reduces to the ionosphere-fixed model (treating the ionospheric corrections deterministically), while when the ionospheric standard deviation approaches infinity, the ionosphere-weighted model reduces to the ionosphere-float model (treating the ionospheric delays as completely unknown parameters; the ionospheric corrections are not used at all), e.g. (Odijk,2000).

Ambiguity resolution consists of two steps. In the first step, the float DD ambiguities are input to the LAMBDA method (Teunissen, 1993-1995) and integer ambiguities are estimated. The LAMBDA method is optimal, since it gives the highest success rate of estimating the correct integers. In this context it is emphasized that our method truly is a multi-frequency approach of ambiguity resolution. Before applying the LAMBDA method, we do not predefine linear combinations (wide lanes or super wide lanes) of phase observables and/or DD ambiguities, as is done in for example Feng and Li (2008) or Cocard et al. (2008). Linear ambiguity transformations are however formed *inside* the LAMBDA method, but this is purely done to improve the numerical efficiency of the integer least-squares search and does *not* alter the ambiguity success rate. It is remarked here that if instead of LAMBDA, one opts for the bootstrapping integer estimation technique (Teunissen, 1998), the decorrelating transformation of the LAMBDA method delivers the optimal ambiguity combination for bootstrapping. After integer estimation using LAMBDA, the Ratio test with fixed failure rate decides whether these integers can be accepted or not. The Fixed Failure (FF) Ratio test differs from the traditional ratio test used in GNSS processing in the sense that no fixed critical value is used (Teunissen and Verhagen, 2007-2009). However, the critical value is set based on the GNSS model at hand such that the probability of accepting a wrong integer solution (i.e. the failure rate) is below a fixed user-defined threshold.

Having obtained an integer ambiguity solution estimated by LAMBDA and accepted by the FFRatio test, the last step of the WARTK user's processing is the computation of the fixed baseline solution, again based on the ionosphere-weighted model, with the only difference being that the integer ambiguities are fixed.

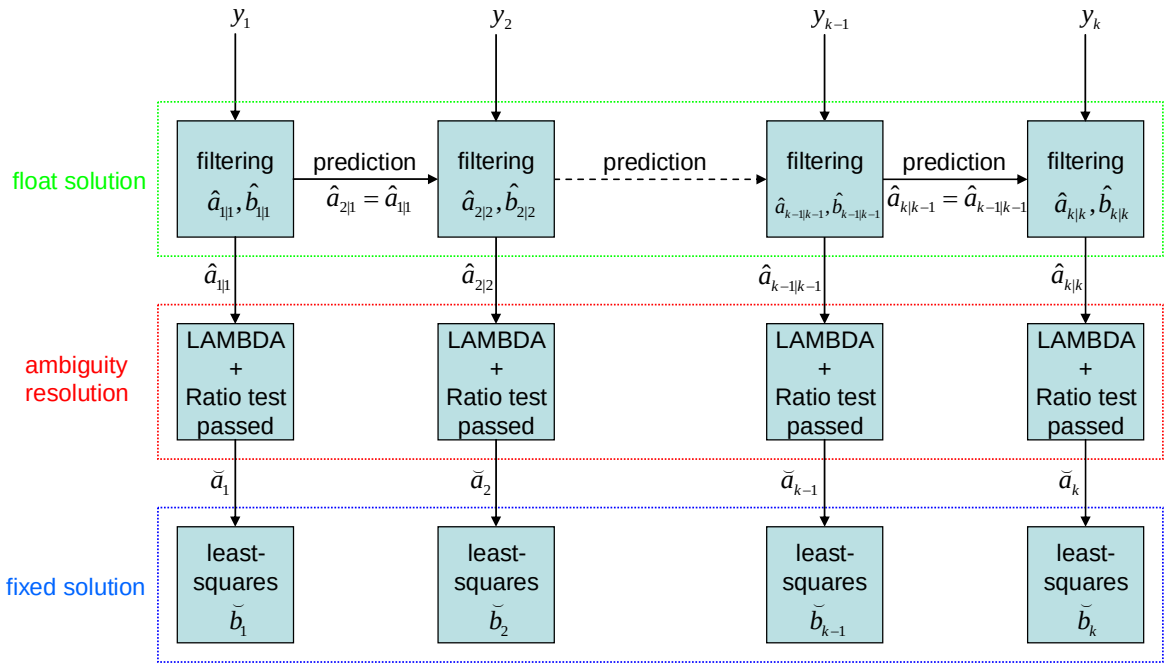

Figure 2 Schematic overview of the multi-epoch processing strategy: Kalman filtering of float solution, where the float ambiguities are 'predicted' to the next epoch (time update). For each epoch the float ambiguities are input for the LAMBDA method and FFRatio test. If this ratio test is passed, the fixed baseline solution is computed by means of least-squares.

The above three-step procedure (float solution–ambiguity resolution–fixed solution) is implemented in two ways. First, as to test the performance of *instantaneous* ambiguity resolution, the processing can be carried out on an epoch-by-epoch basis. This means that the LAMBDA method and FFRatio test are run every epoch, completely irrespective of the outcomes of previous epochs. If this fastest way of ambiguity resolution is not feasible due to the weakness of the model, a *multi-epoch* processing can be carried out, see Figure 2 for a schematic overview. In this multi-epoch processing the float solution is computed per epoch by means of a Kalman filter, which is based on the assumption that the ambiguities remain constant in time (as far as no cycle slips occur). Note that this is the only prediction in the Kalman filter; for all other parameters (baseline, ionospheric delays, etc.) no assumptions are done concerning their dynamics. After initializing the filter at the first epoch by computing a least-squares solution of the ambiguities (denoted as $\hat{a}_{1|1}$) and the other parameters (baseline, ionospheric delays, etc.; denoted as $\hat{b}_{1|1}$), the estimated float ambiguities are 'predicted' forward to the next epoch (the predicted ambiguities of this epoch are denoted as $\hat{a}_{2|1}$). Using the incoming observations of that epoch (denoted as y_2) a 'filtering' step produces new estimates ($\hat{a}_{2|2}$) that are used for the prediction of the following epoch, and so on. Parallel to this Kalman filter implementation, at each epoch the float ambiguities plus their variance-covariance matrix are input to the LAMBDA method and FFRatio test. And, depending on whether the FFRatio test is passed, the fixed solution of the baseline components (and other parameters; denoted by $\breve{b}_{1|1}$) is obtained by means of least-squares. Note that the only difference between this multi-epoch implementation and the epoch-by-epoch processing is the Kalman prediction of the ambiguities. It is remarked that both implementations (Kalman filter as well as the epoch-by-epoch processing), are very suitable to be used in real-time.

3. SIMULATING GALILEO TRIPLE-FREQUENCY WARTK DATA

The Galileo triple-frequency phase and code data have been simulated using the GSVF-2 (Galileo Simulation Validation Facility) at the European Navigation Laboratory at ESA-ESTEC premises in The Netherlands. Galileo System Test Bed (GSTB-V2) signals were generated and the data were tracked and recorded with the Galileo Experimental Test Receiver (GETR) of Septentrio.

The L1BC (overlapping GPS L1), E5a (overlapping GPS L5) and E5b signals have been generated and the collected data (at 1 Hz) were converted to Rinex V3 format. Unfortunately, due to the limited number of available channels of the GETR receiver, which is originally intended for in-orbit validation of Galileo signals transmitted by GSTB-V2 satellites (Simsky et al., 2005), we were able to simulate triple-frequency data of 6 satellites only. This implied that some of the 8-10 satellites that could have been received based on the nominal Galileo constellation had to be removed (see Figure 3, for the resulting sky plot). However the PDOP as based on the 'reduced' 6-satellite geometry was on average still below 2.5, compared to an average of below 2.0 based on the nominal geometry.

To keep the simulations as simple as possible, only static user receivers have been simulated. Galileo data for six reference stations and three user stations have been generated(see Figure 4 for their location). Five reference stations are part of the RIMS network, while reference station STAS (Norway) has been added to fill the gap in the North. The distances between the reference stations are 1300 km at maximum. With station A015 (South England) selected as master reference station the distances to the three user stations are 114 km (HERS), 257 km (DUNK) and 398 km (BRUS).

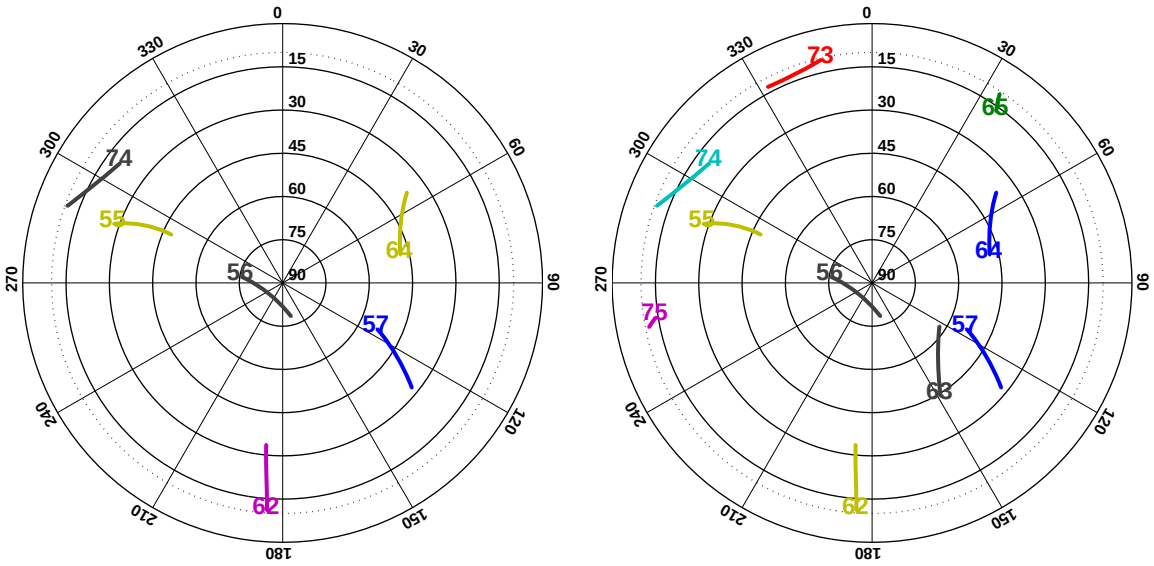

Figure 3 Average Galileo sky plot used for the simulations (left) vs. average Galileo sky plot based on the nominal constellation (right), using a cut-off of 10 deg.

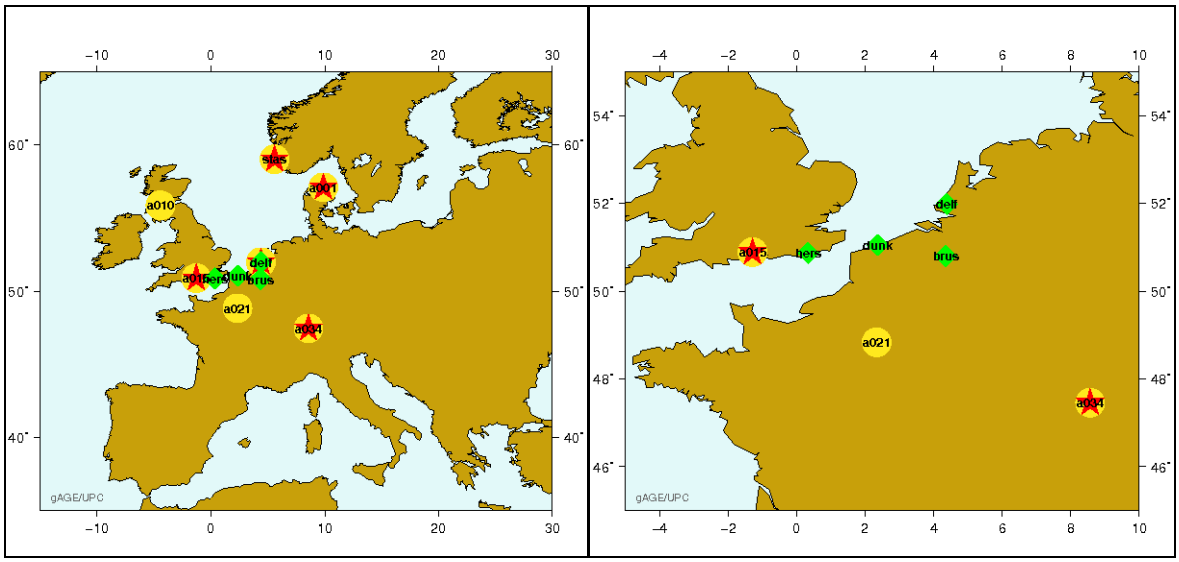

Figure 4 Location of reference stations and roving receivers used in the simulations.

Table 1 summarizes the simulation scenarios. Concerning the transmitted signal power, it was decided to perform two simulations for the rover stations, one based on a *moderate* signal power of 30 dBW and a second based on a *lower* power of 24 dBW. Using these two variants we are able to investigate the effect of the signal-to-noise ratios on the rover's WARTK performance. With respect to the atmospheric contribution, the ionospheric and tropospheric delays have been added to the data *after* the simulations (thus not in the GSVF-2). The generated ionospheric delays are based on the IRI2007 model (Bilitza and Reinisch, 2008) and correspond to 1 January 1999, a day with moderate solar activity. The tropospheric delays have been computed using the modified Hopfield model (Goad and Goodman, 1974), considering a constant value for both the dry and wet zenith tropospheric delays and a mapping function.

Date & time	12 October 2006, 10.30-11.30 UTC
Data sampling interval	1 sec
Galileo signals	L1 (1575.42 MHz), E5a (1176.45 MHz), E5b (1207.14 MHz)
Reference stations	RIMS A010, A021, A001, A015, A034 and STAS
Rover (user) stations	DUNK, HERS, BRUS
Transmitted satellite signal power	Reference stations: normal (30 dBW) Rover stations: moderate (30 dBW) and lower (24 dBW)
Phase ambiguity values	Zero
Satellite clock errors	PRN number × 100 ns
Ionosphere	Moderate activity, based on IRI2007 model
Troposphere	Modified Hopfield model with the following settings: • air pressure: 1014 HPa • temperature: 290 K • relative humidity: 0.31

Table 1 Summary of the simulation scenarios

4. PERFORMANCE OF WARTK USER AMBIGUITY RESOLUTION

At the WARTK processing facility an ionospheric tomography model has been computed from the simulated Galileo data of the RIMS reference stations, based on the procedure described in Colombo et al. (1999) and Hernández-Pajares et al. (2000). Next, the ionospheric

corrections for the user stations are interpolated from the modelled ionospheric delays between the network stations. This interpolation has been carried out by using a planar fit of the ionospheric delays for each satellite from the set of reference stations. Since the ionospheric corrections are not available for the first 13 minutes of the 1 hour time span, all results in this section are based on the remaining 2799 epochs (at 1 sec sampling) for which there are corrections available. In the processing the satellite positions had the same values as were used to generate the Galileo signals.

4.1 DD ionospheric delays in the user baselines before and after WARTK correction

To get insight in the performance of the ionospheric corrections as generated by the WARTK processing facility, for the three user baselines (A015-HERS, A015-DUNK and A015-BRUS) the DD ionospheric delays as present in the simulated data have been plotted in Figure 5, based on float ambiguities as well as with the correct integers fixed (so that the ambiguity-fixed DD ionospheric delays are more precise). Note that the satellite PRN numbers as used in Figure 5 (and also in Figure 6) differ by 100 compared to those used in the sky plots in Figure 3, because our processing software adds this up in case of Galileo satellites. PRN 156 having the highest elevation was selected as reference satellite and hence the DD ionospheric delays are zero. Figure 6 shows for these three baselines the residual DD ionospheric delays after the WARTK ionospheric corrections were applied to the phase and code observations. As can be seen, for all three baselines the WARTK ionospheric corrections are very beneficial, since the residual ionospheric DD delays are significantly lower than the 'true' DD ionospheric delays in the data. Table 2 shows the maximum absolute DD ionospheric delays in the three baselines before and after applying the WARTK ionospheric corrections. Although the residual DD ionospheric delays tend to increase with baseline length, the maximum DD ionospheric error is reduced by a factor of 5-8, depending on the baseline length.

	Max. DD ionospheric delay [m] before WARTK corrections	Max. DD ionospheric delay [m] after WARTK corrections
A015 – HERS (114 km)	0.25	0.05
A015 – DUNK (257 km)	0.62	0.12
A015 – BRUS (398 km)	1.20	0.15

Table 2 Maximum absolute DD ionospheric delay (in m; L1) based on fixed ambiguities.

4.2 WARTK user's ambiguity resolution performance

Next, the benefits of the WARTK ionospheric corrections in terms of enhancing user ambiguity resolution have been investigated. For this purpose, we distinguished between the two simulation scenarios of moderate (30 dBW) and lower signal power (24 dBW). In order to deal with the noisier conditions in case of lower signal power, the standard deviations of the triple-frequency phase and code observations have been set a factor 1.5 larger than in case of moderate signal power. Table 3 summarizes the applied standard deviations in the processing of the user WARTK data. The choices of the ionospheric standard deviation followed from the processing by the WARTK processing facility. Since it was demonstrated that the ionospheric residuals are generally larger for longer baseline lengths, the ionospheric standard deviations are set accordingly. In this context it is recognized that assigning the ionospheric corrections with an *individual* standard deviation as a function of satellite and epoch is a more refined approach than the one applied here, based on a fixed value per baseline, but this approach has not been investigated for the current paper.

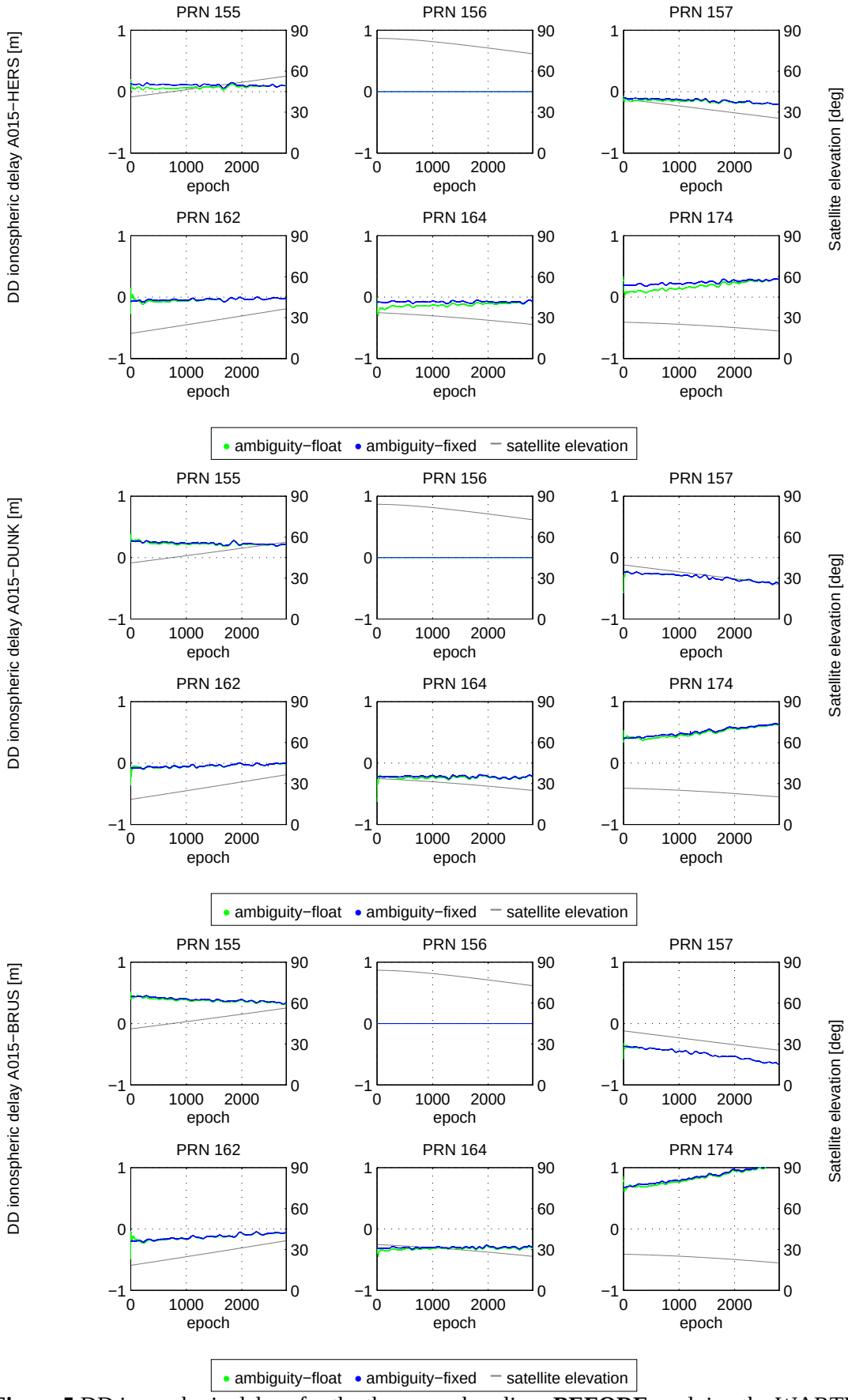

Figure 5 DD ionospheric delays for the three user baselines **BEFORE** applying the WARTK ionospheric corrections.

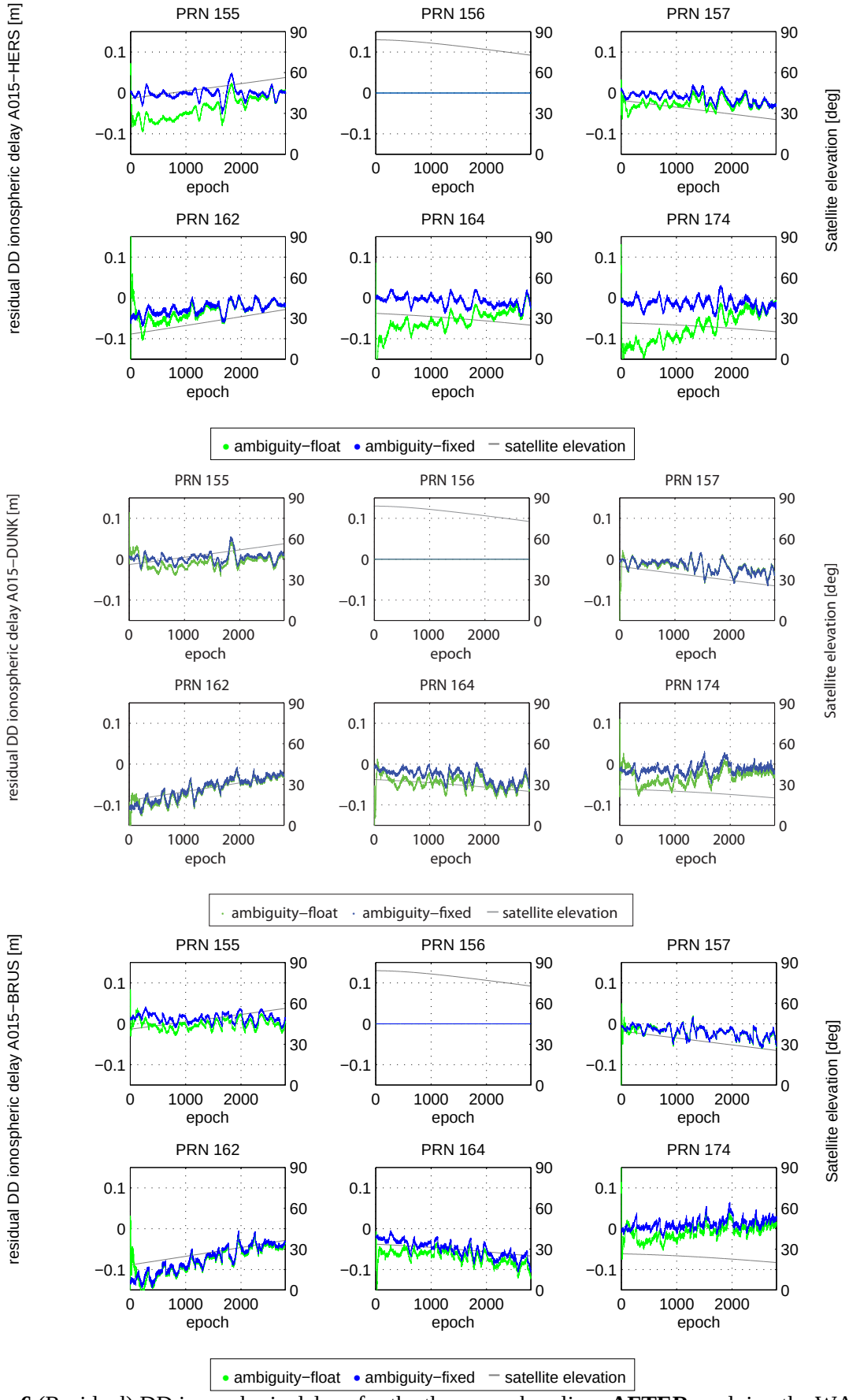

Figure 6 (Residual) DD ionospheric delays for the three user baselines **AFTER** applying the WARTK ionospheric corrections.

Signal power	Phase standard deviations	Code standard deviations	Ionosphere standard deviation
Moderate (30 dBW)	L1: 1 mm E5a: 1 mm E5b: 1 mm	C1: 10 cm C5a: 5 cm C5b: 4 cm	HERS: 1 cm DUNK: 3 cm BRUS: 5 cm
Lower (24 dBW)	L1: 1.5 mm E5a: 1.5 mm E5b: 1.5 mm	C1: 15 cm C5a: 7.5 cm C5b: 6 cm	

Table 3 Standard deviation settings for WARTK user processing. Note: all standard deviations are undifferenced. The ionospheric standard deviation applies to the L1 frequency.

A priori tropospheric corrections are computed using Saastamoinen's model. Although the simulated data correspond to static receivers, in the user's processing these data are processed in a kinematic way, i.e. for each epoch a new rover position will be estimated.

For each of the two signal power scenarios we first performed an epoch-by-epoch processing to investigate the feasibility of instantaneous ambiguity resolution. In case this turns out to be infeasible, the data were processed using the Kalman filter implementation as described in Section 3. In addition, with regard to the treatment of the ionosphere for each scenario an ionosphere-weighted as well as an ionosphere-float processing was conducted. Although the ionosphere-float processing does not use the WARTK ionospheric corrections (it basically estimates the ionospheric delays from the phase and code data) and is not expected to deliver fast ambiguity resolution, its performance is analysed here to assess the minimal observation time needed to fix the ambiguities compared to an ionosphere-weighted processing. Finally, for all scenarios we also did a dual-frequency processing, based on the L1 and E5a frequencies, to assess the benefits of a third frequency.

		Ionosphere-weighted		Ionosphere-float	
		L1+E5a	L1+E5a+E5b	L1+E5a	L1+E5a+E5b
A015-HERS (114 km)	Instantaneous AR success rate	99.9%	99.9%	0%	0%
	Mean TTFFA	0 sec	0 sec	50 sec	15 sec
A015-DUNK (257 km)	Instantaneous AR success rate	36.4%	43.9%	0%	0%
	Mean TTFFA	5 sec	5 sec	75 sec	15 sec
A015-BRUS (398 km)	Instantaneous AR success rate	4.6%	8.6%	0%	0%
	Mean TTFFA	25 sec	10 sec	100 sec	25 sec

Table 4 WARTK user ambiguity resolution results for the **moderate** signal power scenario.

		Ionosphere-weighted		Ionosphere-float	
		L1+E5a	L1+E5a+E5b	L1+E5a	L1+E5a+E5b
A015-HERS (114 km)	Instantaneous AR success rate	99.7%	99.7%	0%	0%
	Mean TTFFA	0 sec	0 sec	50 sec	25 sec
A015-DUNK (257 km)	Instantaneous AR success rate	11.5%	11.8%	0%	0%
	Mean TTFFA	5 sec	5 sec	75 sec	50 sec
A015-BRUS (398 km)	Instantaneous AR success rate	0.2%	1.1%	0%	0%
	Mean TTFFA	75 sec	50 sec	150 sec	75 sec

Table 5 WARTK user ambiguity resolution results for the **lower** signal power scenario.

The results of the different WARTK processing schemes for the three simulated user baselines are summarized in Tables 4 and 5. It is mentioned that "Instantaneous AR success rate" refers to the number of epochs for which the FFRatio tests are passed and at the same time the correct integer ambiguities are estimated by LAMBDA, relative to the total number of epochs (2799, at 1 sec sampling interval). In addition, the "mean Time-Time-To-First-Fix-Ambiguities (TTFFA)" is the average time the Kalman filter needs before the correct integer ambiguities are estimated by LAMBDA and accepted by the Ratio test. To compute this average, the time span of 2799 sec was divided into equal time windows that do not overlap, where it was for varying window lengths checked at which length the correct integers were obtained. For all scenarios we have used a fixed failure rate of 0.001 to execute the FFRatio tests.

Concerning the performance of instantaneous ambiguity resolution, from Tables 4 and 5 it follows that this is almost 100% for the 114-km baseline in both scenarios if the ionospheric corrections are weighted. In this context we remark that the performance of instantaneous ambiguity resolution based on the ionosphere-fixed model (so setting the standard deviations of the ionospheric corrections to zero) are significantly worse: 89.1% for dual-frequency and 90.8% for triple-frequency, both for the 114-km baseline under the moderate signal power conditions (note that these ionosphere-fixed results are not shown in the tables). This demonstrates that weighting the ionospheric corrections is beneficial. The ionosphere-weighted success rate for this shortest baseline is already at a very high level using dual-frequency data only (99.7% in case of the lower signal power and 99.9% in case of moderate signal power), so for this baseline a third frequency does not add improvement. For the two longer baselines the instantaneous success rates are much lower than for the 114-km baseline, even close to zero for the 398-km baseline using the noisier data. For these baselines the quality of the ionospheric corrections is less, weakening the float solution and ambiguity resolution. Increasing the time to resolve the ambiguities for these two baselines improves the reliability of ambiguity resolution significantly: for the 257-km baseline it is possible to fix the ambiguities within only 5 sec, while for the 398-km this becomes feasible within 50 sec, based on triple-frequency data, see Table 5. In addition, the results for the longest baseline indicate that adding a third frequency is beneficial in terms of TTFFA.

If the WARTK ionospheric corrections are not used at all for these three long baselines, i.e. performing an ionosphere-float processing, it follows from Tables 4 and 5 that instantaneous ambiguity resolution is impossible. However, increasing the time to fix the ambiguities is very beneficial here: even for the longest 398-km baseline the ambiguities can be resolved within 25 sec, based on triple-frequency data under moderate signal power conditions (see Table 4) and within 75 sec under poorer signal power conditions (see Table 5). For the ionosphere-float processing strategy a third frequency reduces the TTFFA by a factor of 3-5 compared to dual-frequency, in the moderate signal power scenario. With lower signal powers, the benefit of a third frequency becomes less; the improvement is a factor of 1-2.

4.2 WARTK user's positioning performance

After ambiguity resolution, the WARTK user's positions are estimated by keeping the integer ambiguities fixed. To get insight in the final coordinate precision, Table 6 presents for station BRUS, at 398 km from reference station A015, the 95% Horizontal and Vertical Position Errors (HPEs and VPEs) with the ambiguities float as well as (correctly) fixed. These errors are computed by comparing the estimated positions with the exactly known user positions.

We only present here the results for user station BRUS of the Kalman filter processing based on dual-frequency data, because the results for the other user stations are all (slightly) better. So these position errors can be regarded as upper bounds for our computations. As can be seen from Table 6, WARTK ambiguity resolution has a significant impact on the positioning accuracy: the coordinates improve by a factor of 2-25 when comparing the float and fixed errors. The 95% fixed horizontal position errors are all below 1.5 cm, while their vertical counterparts are at most 2.0 cm.

Signal power	Ionosphere-weighted				Ionosphere-float			
	HPE (95%)		VPE (95%)		HPE (95%)		VPE (95%)	
	Float	Fixed	Float	Fixed	Float	Fixed	Float	Fixed
Moderate (30 dBW)	15.0 cm	0.8 cm	19.8 cm	1.6 cm	23.1 cm	0.9 cm	36.7 cm	1.4 cm
Lower (24 dBW)	15.9 cm	1.3 cm	18.5 cm	2.0 cm	32.0 cm	1.4 cm	33.9 cm	1.8 cm

Table 6 WARTK dual-frequency (L1+E5a) 95% user positioning errors for BRUS.

5. CONCLUSIONS

In this paper simulated Galileo data have been used to assess the performance of high-precision carrier-phase based positioning within a Wide Area RTK network providing ionospheric corrections to users. The following conclusions are drawn.

First, it has been demonstrated that instantaneous LAMBDA-based full ambiguity resolution is feasible for a 114 km WARTK user baseline, already using dual-frequency L1-E5a Galileo data and weighting (with a 1 cm standard deviation) of the ionospheric corrections. However, instantaneous ambiguity resolution is not possible for the longer baselines within the presented simple strategy of ionospheric weighting adopted in this work, taking into account the lower quality of the ionospheric corrections as function of the baseline length. Increasing the time span to at most 75 sec yields successful ambiguity resolution for the user baselines processed here. After full ambiguity resolution the fixed 95% positioning accuracy is below 2 cm for all investigated baselines.

The simulations as described in this paper further demonstrated that addition of a third frequency does not help ambiguity resolution much (compared to dual frequency) in case precise ionospheric corrections are available; although with less accurate ionospheric corrections or even in absence of such WARTK corrections (ionosphere-float processing), the addition of a third frequency reduces the mean TTFFA up to a factor of 5.

Finally we remark that the success rate of triple-frequency Galileo full ambiguity resolution will likely be higher than of future triple-frequency GPS, since the Galileo signals are expected to be more precise than their GPS counterparts. Galileo dual-frequency (L1+E5a) is expected to yield higher success rates than current dual-frequency GPS (L1+L2) because of the more favourable satellite constellation and the lower code noise.

ACKNOWLEDGEMENTS

The major part of this work has been performed under ESA contract in the FES-WARTK project, carried out by Delft University of Technology, The Netherlands, and leaded by the Research Group of Astronomy and Geomatics of the Technical University of Catalonia

(gAGE/UPC) in Spain.

At the time of the project the first author was working as a researcher at Delft University of Technology. Professor Peter J.G. Teunissen is the recipient of an Australian Research Council Federation Fellowship (project number FF0883188). This support is greatly acknowledged. The research of Sandra Verhagen is supported by the Dutch Technology Foundation STW, applied science division of NWO and the Technology Program of the Dutch Ministry of Economic Affairs.

REFERENCES

Bilitza D and Reinisch BW (2008) International Reference Ionosphere 2007: Improvements and new parameters, *Advances in Space Research* 42: 599-609.

Cocard M, Bourgon S, Kamali O, Collins P (2008) A systematic investigation of optimal carrier-phase combinations for modernized triple-frequency GPS, *Journal of Geodesy* 82: 555-564.

Colombo OL, Hernández-Pajares M, Juan JM, Sanz J and Talaya J (1999) Resolving carrier-phase ambiguities on-the-fly, at more than 100 km from nearest site, with the help of ionospheric tomography, *Proc. ION GPS-99*, Nashville, TN, 14-17 September 1999.

Euler HJ, Keenan R, Zebhauser B, Wubbena G (2001), Study of a simplified approach of utilizing information from permanent reference station arrays, *Proc. ION GPS-2001,* Salt Lake City, UT, 11-14 September 2001.

Feng Y, Li B (2008) Three carrier ambiguity resolution: Generalised problems, models, methods and performance analysis using semi-generated triple frequency GPS data, *Proc. ION GNSS-2008,* Savannah, GA, 16-19 September 2008, pp. 2831-2840.

Goad CC and Goodman L (1974) A modified Hopfield tropospheric refraction correction model, *Proc. Fall Annual Meeting of the AGU*, San Francisco, CA, 12-17 December 1974.

Hernández-Pajares M, Juan JM, Sanz J and Colombo OL (2000), Application of ionospheric tomography to real-time GPS carrier-phase ambiguities resolution, at scales of 400-1000 km and with high geomagnetic activity, *Geophysical Research Letters*, Vol. 27, No. 13, pages 2009-2012, July 1, 2000.

Hernández-Pajares M, Juan JM, Sanz J, Orus R, Garcia-Rodriguez A and Colombo OL (2004) Wide Area Real Time Kinematics with Galileo and GPS signals, *Proc. ION GNSS-2004*, Long Beach, CA, 21-24 September 2004, pp. 2541-2554.

Hernández-Pajares M, Juan JM, Sanz J, Aragon-Angel A, Ramos-Bosch P, Odijk D, De Bakker PF, Van der Marel H, Verhagen S, Fernandez- Hernández I, Toledo M and Samson J (2008) Feasibility study of a European Wide Area Real Time Kinematic system, *Proc. NAVITEC '08*, Noordwijk, The Netherlands, CDROM.

Odijk D (2000) Weighting ionospheric corrections to improve fast GPS positioning over medium distances, *Proc. ION GPS-2000*, Salt Lake City, UT, 19-22 September 2000, pp. 1113-1123.

Simsky A, Sleewaegen JM, De Wilde W, Wilms F (2005) Galileo receiver development at Septentrio, *Proc. ENC-GNSS 2005*, Munich, Germany, 19-22 July 2005, CD-ROM.

Simsky A, Sleewaegen JM, Hollreiser M, Crisci M (2006) Performance assessment of Galileo ranging signals transmitted by GSTB-V2 satellites, *Proc. ION GNSS-2006*, Fort Worth, TX, 26-29 September 2006, pp. 1547-1559.

Teunissen PJG (1993) *Least-squares estimation of the integer GPS ambiguities*, Invited lecture, Section IV Theory and Methodology, IAG General Meeting, Beijing, China, August 1993.

Teunissen PJG (1995) The least-squares ambiguity decorrelation adjustment: a method for fast GPS integer ambiguity estimation, *Journal of Geodesy* 70: 65-82.

Teunissen PJG (1998) Success probability of integer GPS ambiguity rounding and bootstrapping, *Journal of Geodesy* 72: 606-612.

Teunissen PJG, Verhagen S (2007) On GNSS ambiguity acceptance tests, *Proc. IGNSS 2007*, Sydney, Australia, 4-6 December 2007, CD-ROM.

Teunissen PJG, Verhagen S (2009) The GNSS ambiguity ratio-test revisited, *Survey Review 41(312),* pp. 138-151.

Verhagen S, Teunissen PJG, Odijk D (2007) Carrier-phase ambiguity success rates for integrated GPS-Galileo satellite navigation, *Proc. SANE2007, IEICE, Japan,* Vol. 107, No. 2, pp. 139-144.

Vollath U, Deking A, Landau H, Pagels C, Wagner B (2000), Multi-base RTK positioning using Virtual Reference Stations, *Proc. ION GPS-2000,* Salt Lake City, UT, 19-22 September 2000.